On the Behavior of Communication Links of a Node in a Multi-Hop Mobile Environment

Prince Samar and Stephen B. Wicker
School of Electrical and Computer Engineering
Cornell University, Ithaca, NY 14853
{samar, wicker}@ece.cornell.edu

ABSTRACT

In this work, we develop an analytical framework to investigate the behavior of the communication links of a node in a random mobility environment. Analytical expressions characterizing various properties related to the formation, lifetime and expiration of links are derived. The derived framework can be used to design efficient algorithms for medium access, routing and transport control, or to analyze and optimize the performance of existing network protocols. A number of applications of the characteristics investigated, such as selection of stable routes, route cache lifetime optimization, providing Quality-of-Service (QoS) data communication and analysis of route lifetime are discussed. In particular, we focus on designing an efficient updating strategy for proactive routing protocols based on the derived statistics. Using simulations, we show that the proposed strategy can lead to significant performance improvements in terms of reduction in routing overhead, while maintaining high data packet delivery ratio and acceptable latency.

Categories and Subject Descriptors

C.2.1 [**Computer-Communication Networks**]: Network Architecture and Design; C.2.2 [**Computer-Communication Networks**]: Network Protocols

General Terms

Algorithms, Design, Performance, Theory

Keywords

Ad hoc networks, mobility, communication link, link dynamics, lifetime, interarrival time, proactive routing, updating

1. INTRODUCTION

As ad hoc and sensor networks do not require any pre-existing infrastructure and are self-organizing as well as self-configuring, they are amenable to a multitude of applica-

tions in diverse environments. These include battlefield deployments, where the transceivers may be mounted on Unmanned Aerial Vehicles (UAVs) flying overhead, on moving armored vehicles or may be carried by soldiers on foot. They may be used for communication during disaster relief efforts or law enforcement operations in hostile environment. Such networks may be set up between students in a classroom or delegates at a convention center. Chemical, biological or weather-related sensors may be spread around on land or on flotation devices at sea to monitor the environment and convey related statistics. Sensors may even be mounted on animals (e.g., whales, migratory birds and other endangered species) to collect biological and environmental data.

With such a varied range of applications envisioned for ad hoc and sensor networks, the nodes in the network are expected to be mobile. Due to limited transmission range, this implies that the set of communication links of a particular node may undergo frequent changes. These changes in the set of links of a node affect not only the node's ongoing communication, but may impede the communication of other nodes as well, due to the distributed, multi-hop nature of such networks.

As the capacity and communication ability of ad hoc and sensor networks are dependent on the communication links [8], it is important to understand how the links of a node behave in a mobile environment. In this paper, we will analyze the dynamics of communication links of a node. The aim of the study is to gain an understanding of how the links behave and their properties vary depending on the network characteristics. The intuition developed can then be applied to design effective protocols for ad hoc and sensor networks.

The contributions of this paper are threefold. Firstly, we develop a theoretical framework to study the means and the distributions of link lifetime, new link interarrival time, link breakage interarrival time and link change interarrival time. Further, the techniques employed could be used to study the statistics of link properties in other settings as well. Secondly, the theoretical framework developed can not only help analyze and optimize existing network protocols, but can also assist in the design of efficient algorithms for medium access, routing and transport control. We outline a number of applications of the derived properties in section 5. Lastly, to provide an illustration, we design an efficient updating strategy for proactive routing protocols using the derived properties and show that it leads to significant performance improvements.

The rest of the paper is organized as follows. In section 2, we discuss related work on characterizing the link behav-

ior in an ad hoc or sensor network. Various properties of the links of a node in a mobile environment are derived in section 3. In section 4, we validate the derived expressions with simulation results. Some applications of the derived properties are discussed in section 5. In section 6, we design and evaluate an updating strategy for proactive routing protocols. Finally, section 7 concludes the paper.

2. RELATED WORK

Simulation has been the primary tool utilized in the literature to characterize and evaluate link properties in ad hoc and sensor networks. Some efforts have been directed at designing routing schemes that rely on identification of stable links in the network. Nodes make on-line measurements (about beacons or signal strength received from a neighbor) in order to categorize stable links, which are then preferentially used for routing. Examples are Associativity-Based Routing (ABR) [25], Signal Strength-based Adaptive Routing (SSA) [6] and Route-lifetime Assessment Based Routing (RABR) [1]. However, these approaches suffer from the fact that a link deemed stable based on past or current measurements may soon become unreliable (as compared to those currently categorized as unstable), due to the dynamic nature of mobile wireless environments.

Empirical distributions of link lifetime and residual link lifetime have been presented in [7] by running simulations for different parameter values. [20] also uses simulations to study the probability densities of link lifetime and route lifetime for some mobility models. In [24], a node relies on the availability of a Global Positioning System to provide information about the current positions and velocities of the node and its neighbor in order to predict the link expiration time. Estimated stability of links has been used as the basis of route caching strategies for reactive routing protocols [12].

Analytical study of link characteristics in a mobile network has been limited, partly due to the abstruse nature of the problem. Though a number of mobility models have been proposed and used in the literature [5], none of them is satisfactory for representing node mobility in general. The commonly used *random waypoint* mobility model has been studied in [3] and [4] to investigate certain mobility properties like transition length and time of a mobile node between two waypoints, the direction angle at the beginning of a movement transition and the spatial distribution of nodes. It has been found that the random waypoint model leads to non-uniform spatial distribution of nodes such that there is a higher concentration of nodes towards the center of the network region than close to the boundaries. Further, the model could lead to unreliable results as it fails to give a steady state, with the average nodal speed consistently decreasing over time [27].

The expected lifetime of a link is examined in [26] for some simple mobility scenarios like deterministic mobility and Brownian motion. A random mobility model has been developed in [15], which is then used to quantify the probability that a link will be available between two nodes after an interval of duration t, given that the link exists between them at time t_0. However, the model considers a link to be available at time $t_0 + t$ even when it undergoes failure during one or more intervals between t_0 and $t_0 + t$. [13] tries to overcome this drawback by estimating the probability that a link between two nodes will be continuously available for a certain period T_p, where T_p is predicted based on the nodes'

current movements. Approximations to the distribution of link distances within a rectangular region are presented in [16], assuming that the x and y node coordinates follow independent continuous spatial distributions.

Although these works shed some light, many important issues related to the behavior of links remain largely unexplored. In this paper, we develop an analytical framework in order to investigate characteristics related to the creation, lifetime and expiration of links in a mobile environment. To the best of the authors' knowledge, such a study at this level has not been done before. As will be seen later, the derived link properties can be instrumental in the design and analysis of networking algorithms.

3. LINK PROPERTIES

Here, we derive analytical expressions for a number of link properties: (a) expected lifetime of a link, (b) probability distribution of link lifetime, (c) expected rate of new link arrivals, (d) probability distribution of new link interarrival time, (e) expected rate of link breakages, (f) probability distribution of link breakage interarrival time, (g) expected rate of link changes, and (h) probability distribution of link change interarrival time. These expressions will help us better understand the behavior of communication links and their dependence on various network parameters.

In order to model the network for the analyses, we make the following assumptions.

1. A node has a bidirectional communication link with any other node within a distance of R meters from it. The link breaks if the node moves to a distance greater than R.

2. A node in the network moves with a constant velocity which is uniformly distributed between a meters/second and b meters/second.

3. The direction of a node's velocity is uniformly distributed between 0 and 2π.

4. A node's speed, its direction of motion and its location are mutually independent.

5. The initial locations of nodes in the network are modeled by a two-dimensional *Poisson Process* with intensity σ such that for a network region **D** with an area A, the probability that **D** contains k nodes is given by

$$Prob(k \ nodes \ in \ \mathbf{D}) = \frac{(\sigma A)^k e^{-\sigma A}}{k!} \qquad (1)$$

Assumption 1 implies that the Signal to Interference Ratio (SIR) remains high up to a certain distance R from the transmitter, enabling nearly perfect estimation of the transmitted signal. However, SIR drops beyond this distance, rapidly increasing the bit error rate (BER) to unacceptable levels. Though the shadow and multipath fading experienced by the received signal may make the actual transmission zone unsymmetrical, this is a fair approximation if all the nodes in the network use the same transmission power. This simplifying assumption is commonly used in the simulation and analysis of ad hoc and sensor networks.

Assumption 2 models a mobile environment where nodes are moving around with different velocities that are uniformly distributed between two limits. This high mobility

model is chosen as it is challenging for network communication and can, thus, facilitate finding "worst-case" bounds on the link properties for a general scenario. It is to be noted that the intensity of mobility being modeled can be changed by appropriately choosing the two parameters, a and b.

Assumptions 2-5 characterize the aggregate behavior of nodes in a large network. Due to the large number of independent nodes operating in an ad hoc fashion, any correlation between nodes can be assumed to be insignificant. Although it is possible that some nodes may share similar objectives and may move together, a large enough population of autonomous nodes can be expected in the network so that the composite effect can be modeled by a random process.

Note that Assumption 5 indicates the location distribution of nodes in the network at the start, as well as at any later point of time. This is because the node velocities are independent of the node locations, leading to a uniform distribution of the node locations at any point of time. Poisson processes model "total randomness," thus reflecting the randomness shown by the aggregate behavior of nodes in a large network. This assumption is frequently used to model the location of nodes in an ad hoc or cellular network. Using (1), it is easy to see that the expected number of nodes in **D** is equal to σA. Thus, σ represents the average density of nodes in the network.
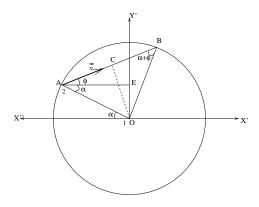
3.1 Expected Link Lifetime

Figure 1: The transmission zone of node 1 at O with node 2 entering the zone at A and exiting at B.

Figure 1 shows the transmission zone of a node (say node 1) which is a circle of radius R centered at the node. The figure shows the trajectory of another node (say node 2) entering the transmission zone of node 1 at A, traveling along AB, and exiting the transmission zone at B.

With respect to a stationary Cartesian coordinate system with orthogonal unit vectors $\hat{i}$ and $\hat{j}$ along the X and Y axes respectively, let the velocity of node 1 be $\vec{v}_1 = v_1\hat{i}$ and the velocity of node 2, which makes an angle θ with the positive X axis, be $\vec{v}_2 = v_2\cos\theta\hat{i} + v_2\sin\theta\hat{j}$. Hence, the relative velocity of node 2 with respect to node 1 is

$$\vec{v} \triangleq \vec{v}_{21} = \vec{v}_2 - \vec{v}_1 = (v_2\cos\theta - v_1)\hat{i} + v_2\sin\theta\hat{j} \quad (2)$$

Consider a Cartesian coordinate system $X'Y'$ fixed on node 1 such that the X' and Y' axes are parallel to $\hat{i}$ and $\hat{j}$ respectively, as shown in Figure 1. The magnitude of node

2's velocity in this coordinate system is

$$v \triangleq |\vec{v}| = \sqrt{v_1^2 + v_2^2 - 2v_1 v_2\cos\theta} \quad (3)$$

and its direction of motion in this coordinate system, as indicated in Figure 1, is

$$\phi \triangleq \angle\vec{v} = \tan^{-1}\left(\frac{\sin\theta}{\cos\theta - v_1/v_2}\right) \quad (4)$$

Let node 2's point of entry A in node 1's transmission zone be defined by an angle α, measured clockwise from OX''. Thus, point A has coordinates $(-R\cos\alpha, R\sin\alpha)$ in the $X'Y'$ coordinate system. In Figure 1, $OA = OB = R$. AB makes an angle ϕ with the horizontal, which is the direction of the relative velocity of node 2. Line OC is perpendicular to AB. As OAB makes an isosceles triangle, $\angle OAB = \angle OBA = \alpha + \phi$. Therefore, $AC = BC = R\cos(\alpha + \phi)$. As θ and ϕ can have any value between 0 and 2π, the distance d_{link} that node 2 travels inside node 1's zone is

$$d_{link} = |2R\cos(\alpha + \phi)| = 2R|\cos(\alpha + \phi)| \quad (5)$$

Hence, the time that node 2 spends inside node 1's zone, which is equal to the time for which the link between node 1 and node 2 remains active, is

$$t_{link} = \frac{2R|\cos(\alpha + \phi)|}{v} \quad (6)$$

The mean link lifetime of node 1 as a function of its velocity v_1 can be calculated as the expectation of t_{link} over v, ϕ, α.

$$\bar{T}_{link}(v_1) = E_{v\phi\alpha}\big[t_{link}\big] \quad (7)$$

Let the joint probability density function of v, ϕ, α for nodes that enter the zone be $f_{v\phi\alpha}(v, \phi, \alpha)$. It can be expressed as

$$f_{v\phi\alpha}(v, \phi, \alpha) = f_{\alpha|v\phi}(\alpha|v, \phi)f_{v\phi}(v, \phi) \quad (8)$$

where $f_{\alpha|v\phi}(\alpha|v, \phi)$ is the conditional probability density of α given the relative velocity $\vec{v}$; and $f_{v\phi}(v, \phi)$ is the joint probability density of the magnitude v and phase ϕ of $\vec{v}$. They can be expressed as (see [23])

$$f_{\alpha|v\phi}(\alpha|v, \phi) = \frac{1}{2}\cos(\alpha + \phi)\bigg\{u\Big(\alpha + \big(\frac{\pi}{2} + \phi\big)\Big)$$
$$- u\Big(\alpha - \big(\frac{\pi}{2} - \phi\big)\Big)\bigg\} \quad (9)$$

$$f_{v\phi}(v, \phi) = \frac{1}{2\pi(b - a)}vg(v, \phi, v_1) \quad (10)$$

where

$$g(v, \phi, v_1) = \frac{u\big(h(v, \phi, v_1) - a\big) - u\big(h(v, \phi, v_1) - b\big)}{h(v, \phi, v_1)} \ , \quad (11)$$

$$h(v, \phi, v_1) = \sqrt{v^2 + v_1^2 + 2vv_1\cos\phi} \quad (12)$$

and $u(\cdot)$ is the standard unit step function.

Thus, the expected link lifetime as a function of node velocity v_1 can be evaluated as

$$\bar{T}_{link}(v_1) = \int_0^\infty \int_{-\pi}^\pi \int_{-\pi}^\pi t_{link}f_{v\phi\alpha}(v, \phi, \alpha)d\alpha d\phi dv \quad (13)$$

Using (6), (8), (9) and (10) to simplify (13), we get

$$
\bar{T}_{link}(v_1) = \frac{R}{2(b-a)} \left(\int_0^\pi \log \left| \frac{b + \sqrt{b^2 - v_1^2 \sin^2 \phi}}{v_1 + v_1 \cos \phi} \right| d\phi \right.
$$
$$
\left. - \int_{\phi_0}^\pi \log \left| \frac{a + \sqrt{a^2 - v_1^2 \sin^2 \phi}}{a - \sqrt{a^2 - v_1^2 \sin^2 \phi}} \right| d\phi \right)
$$
(14)

where $\phi_0 = \pi - sin^{-1}(\frac{a}{v_1})$. For the case when the lower bound on the node velocity $a = 0$, the second term in (14) vanishes.

(14) cannot be further integrated into an explicit function. However, it can be numerically integrated to give the expected link lifetime for the chosen distribution of mobility in the network.
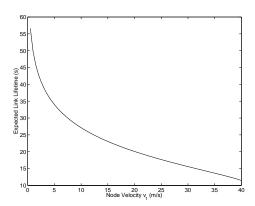

Figure 2: **Expected Link Lifetime of a node as a function of its velocity v_1.**

Figure 2 plots the expected link lifetime for a node as a function of its velocity. The velocity of the nodes in the network is assumed to be uniformly distributed between $[0, 40]$ $meters/second$ and R equals 250 $meters$. As can be observed from the plot, the expected link lifetime for a node decreases rapidly as its velocity is increased. As an illustration, links last almost 3 times longer, on average, for a node moving with a velocity of 5 $meters/second$ as compared to a node moving with a velocity of 40 $meters/second$. Also, as can be seen from (14), the expected link lifetime is directly proportional to the transmission radius R of a node.

It is to be noted that Assumption 5 was not needed for determining the expected link lifetime and, thus, the derived expression is independent of the density of nodes in the network. This is because $\bar{T}_{link}(v_1)$ is averaged over link lifetimes corresponding to the range of velocities present in the network weighted by their probability density, without regard to how many or how often these links are formed.

3.2 Link Lifetime Distribution

For a particular node moving with a velocity v_1, the cumulative distribution function (CDF) of the link lifetime is defined as

$$
F_{link}^{v_1}(t) = Prob\{t_{link} \le t\}
$$
(15)

Clearly, $F_{link}^{v_1}(t) = 0$ for $t < 0$. For $t \ge 0$, we have

$$
F_{link}^{v_1}(t) = Prob\left\{ \frac{2R|\cos(\alpha + \phi)|}{v} \le t \right\}
$$
$$
= 1 - Prob\left\{ |\cos(\alpha + \phi)| > \frac{vt}{2R} \right\}
$$
(16)

Now,

$$
Prob\left\{ |\cos(\alpha + \phi)| > \frac{vt}{2R} \right\}
$$
$$
= \int_{\phi=-\pi}^\pi \int_{v=0}^{\frac{2R}{t}} \int_{\alpha=-cos^{-1}(\frac{vt}{2R})-\phi}^{cos^{-1}(\frac{vt}{2R})-\phi} f_{v\phi\alpha}(v, \phi, \alpha) d\alpha dv d\phi
$$
(17)

Using the expression of $f_{v\phi\alpha}(v, \phi, \alpha)$ from (8) and (17), (16) can be simplified to give the link lifetime CDF for a node moving with velocity v_1.

$$
F_{link}^{v_1}(t)
$$
$$
= 1 - \frac{1}{\pi(b-a)} \int_0^\pi \int_0^{\frac{2R}{t}} v \sqrt{1 - \left(\frac{vt}{2R} \right)^2} g(v, \phi, v_1) dv d\phi
$$
(18)

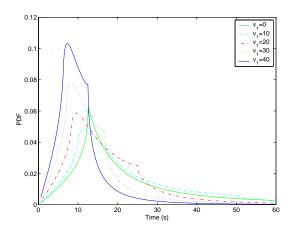where $g(v, \phi, v_1)$ is as defined in (11).

Figure 3: **The link lifetime PDF for a node moving with velocity v_1.**

No closed-form solution for the integrals in (18) exists. However, (18) can be numerically integrated to give the cumulative distribution function of the link lifetime for a node moving with velocity v_1. The probability density function (PDF) $f_{link}^{v_1}(t)$ of link lifetime is found by differentiating (18) with respect to t. Figure 3 plots the link lifetime PDF for different node velocities v_1, where $a = 0$ $meters/second$, $b = 40$ $meters/second$ and $R = 250$ $meters$. Note that for $v_1 > 0$, the point where the PDF curve is not differentiable occurs at $t = \frac{2R}{v_1}$, which corresponds to the time taken by a node moving at velocity v_1 to pass through a transmission zone along its diameter. Also, it can be seen that the maxima of the PDF curve, which corresponds to the *mode* of the distribution, shifts towards the left as the node velocity increases. As in section 3.1, the derived expression does not depend on the density or location distribution of nodes in the network.
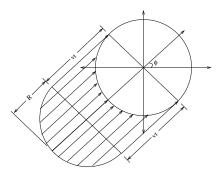
Figure 4: Calculation of expected new link arrival rate.

3.3 Expected New Link Arrival Rate

Consider Figure 4 which shows the transmission zone of node 1 moving with velocity $\vec{v}_1$ with respect to the stationary coordinate system XY, as defined before. For given values of v and ϕ, any node with relative velocity $\vec{v} = v\cos\phi\hat{i} + v\sin\phi\hat{j}$ with respect to node 1 can only enter node 1's transmission zone from a point on the semi-circle $\alpha \in [-(\frac{\pi}{2}+\phi), \frac{\pi}{2}-\phi]$[1]. Thus, a node with relative velocity $\vec{v}$ would enter the transmission zone within the next t seconds if it is currently located in the shaded region $\mathbf{D_a}$ of Figure 4, which is the set of all points at most vt meters away measured along angle ϕ from the semicircle $\alpha \in [-(\frac{\pi}{2}+\phi), \frac{\pi}{2}-\phi]$.

The area of the shaded region $\mathbf{D_a}$ is $A = vt \cdot 2R$. Using Assumption 5, the average number of nodes in $\mathbf{D_a}$ is found to be equal to $2Rvt \cdot \sigma$. Therefore, the average number of nodes in $\mathbf{D_a}$ with velocity $\vec{v}$ is equal to $2R\sigma vt \cdot f(v,\phi)dvd\phi$. This is just the average number of nodes with velocity $\vec{v}$ entering the zone within the next t seconds. The total expected number of nodes entering the zone within the next t seconds, $\eta(v_1)$, is found by integrating this quantity over all possible values of v and ϕ.

$$\eta(v_1) = \int_{v=0}^{\infty}\int_{\phi=-\pi}^{\pi} 2R\sigma vt f(v,\phi)dvd\phi \qquad (19)$$

Thus, the expected number of nodes entering the transmission zone per second, or equivalently, the rate of new link arrivals is given by

$$\dot{\eta}(v_1) = \int_{v=0}^{\infty}\int_{\phi=-\pi}^{\pi} 2R\sigma v f(v,\phi)dvd\phi \qquad (20)$$

$f(v,\phi)$, the joint probability density of a node's relative velocity, is as expressed in (10). Thus (20) can be simplified to give

$$\dot{\eta}(v_1) = \frac{2R\sigma}{\pi(b-a)}\left[b^2\mathcal{E}\left(\frac{v_1}{b}\right) - 2a^2\mathcal{E}\left(\frac{v_1}{a}\right) + a^2\mathcal{E}\left(\phi_0, \frac{v_1}{a}\right)\right.$$
$$+ \frac{v_1^2}{4}\int_0^{\pi} p(\phi)\log\left|\frac{b+\sqrt{b^2-v_1^2\sin^2\phi}}{v_1+v_1\cos\phi}\right|d\phi$$
$$\left.- \frac{v_1^2}{4}\int_{\phi_0}^{\pi} p(\phi)\log\left|\frac{a+\sqrt{a^2-v_1^2\sin^2\phi}}{a-\sqrt{a^2-v_1^2\sin^2\phi}}\right|d\phi\right]$$
$$(21)$$

[1] α, as before, is the angle measured clockwise from the negative X axis of the coordinate system fixed on node 1.

where $\phi_0 = \pi - \sin^{-1}(\frac{a}{v_1})$, $p(\phi) = 1 + 3\cos(2\phi)$, $\mathcal{E}(\cdot)$ is the standard Complete Elliptic Integral of the Second Kind and $\mathcal{E}(\cdot,\cdot)$ is the standard Incomplete Elliptic Integral of the Second Kind. Note that when $a = 0$, only the first and the fourth terms remain – the terms containing a (inside the square brackets) vanish.
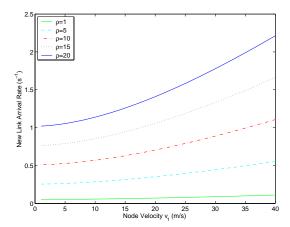

Figure 5: New link arrival rate for a node with velocity v_1.

In Figure 5, we plot the expected rate of new link arrivals for a node moving with velocity v_1. While generating the curves, the values of the parameters are set to $a = 0$ $meters/second$, $b = 40$ $meters/second$, $R = 250$ $meters$ and $\sigma = \frac{\rho}{\pi R^2}$ $nodes/meter^2$. Note that ρ represents the average number of nodes within a transmission zone.

An important point to observe from (21) is that the expected rate of new link arrivals for a node is directly proportional to the average density σ of nodes in the network. It is also directly proportional to the transmission radius R of the nodes.

3.4 New Link Interarrival Time Distribution

The cumulative distribution function of new link interarrival time is defined as

$$F_{arrival}^{v_1}(t) = Prob\{link\ interarrival\ time \leq t\} \qquad (22)$$

$\mathbf{D_a}$, the shaded region of Figure 4, has an area $A = 2Rvt$. As seen in section 3.3, a node with velocity $\vec{v} = v\cos\phi\hat{i} + v\sin\phi\hat{j}$ currently located in $\mathbf{D_a}$ will enter the transmission zone within the next t seconds. Thus, given $\vec{v}$, the probability that the link interarrival time is not more than t is equal to the probability that there exists at least one node in $\mathbf{D_a}$ with velocity $\vec{v}$. Therefore, using Assumption 5,

$$Prob\{link\ interarrival\ time \leq t|v,\phi\}$$
$$= Prob\{at\ least\ 1\ node\ in\ \mathbf{D_a}|v,\phi\}$$
$$= 1 - e^{-2R\sigma tv} \qquad (23)$$

Hence, the cumulative distribution function of new link interarrival time can be expressed as

$$F_{arrival}^{v_1}(t) = \iint_{v,\phi} \left(1 - e^{-2R\sigma tv}\right)f(v,\phi)dvd\phi \qquad (24)$$

149

Substituting for $f(v, \phi)$ from (10) in (24),

$$F_{arrival}^{v_1}(t)$$
$$= 1 - \frac{1}{\pi(b-a)} \int_0^\pi \int_0^\infty v e^{-2R\sigma t v} g(v, \phi, v_1) dv d\phi \tag{25}$$

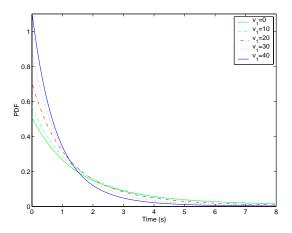where $g(v, \phi, v_1)$ is as defined in (11).

Figure 6: The new link interarrival time PDF for a node with velocity v_1.

The new link interarrival time density, found by differentiating (25), is plotted in Figure 6 for a node with velocity v_1, where $a = 0$ $meters/second$, $b = 40$ $meters/second$, $R = 250$ $meters$ and $\sigma = \frac{10}{\pi R^2}$ $nodes/meter^2$. It can be observed that the new link interarrival time PDF curves drop rapidly as time t increases. In fact, using standard curve fitting techniques, we have found that the new link interarrival time density can be very well approximated by a simple exponential function, with the Root Mean Squared Error (RMSE) for the fit being less than 0.02 for the case in Figure 6.

3.5 Expected Link Change Rate

Any change in the set of links of a node may be either due to the arrival of a new link or due to the breaking of a currently active link. Thus, the expected link change rate for a node is equal to the sum of the expected new link arrival rate and the expected link breakage rate. The expected new link arrival rate is as expressed in (21).

In order to determine the expected link breakage rate, suppose that the network is formed at time $t = 0$. Let the total number of new link arrivals for a node between $t = 0$ and $t = t_0$ be $\eta(t_0)$ and the total number of link breakages for the node during the same interval be $\mu(t_0)$. Let the number of neighbors of the node at time $t = t_0$ be $N(t_0)$. Thus, $\eta(t_0) - \mu(t_0) = N(t_0)$. Dividing both sides by t_0 and taking the limit as $t \to \infty$,

$$\lim_{t \to \infty} \left\{ \frac{\eta(t_0)}{t_0} - \frac{\mu(t_0)}{t_0} \right\} = \lim_{t \to \infty} \frac{N(t_0)}{t_0} \tag{26}$$

Now, $\lim_{t \to \infty} \frac{\eta(t_0)}{t_0}$ equals the expected rate of new link arrivals $\dot{\eta}$ and $\lim_{t \to \infty} \frac{\mu(t_0)}{t_0}$ equals the expected rate of link breakages $\dot{\mu}$ (assuming ergodicity). If the number of neigh-

bors of a node is bounded[2], $\lim_{t \to \infty} \frac{N(t_0)}{t_0} = 0$. This implies that $\dot{\mu} = \dot{\eta}$, i.e., the expected rate of link breakages is equal to the expected rate of new link arrivals. Thus, the expected link change arrival rate $\dot{\gamma}(v_1)$ for a node moving with velocity v_1 is given by

$$\dot{\gamma}(v_1) = \dot{\eta}(v_1) + \dot{\mu}(v_1) = 2\dot{\eta}(v_1) \tag{27}$$
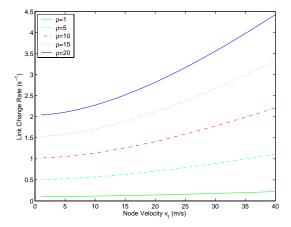
where $\dot{\eta}(v_1)$ is as expressed in (21).

Figure 7: Expected link change rate for a node with velocity v_1.

The expected link change rate as a function of the node velocity v_1 is plotted in Figure 7, where $a = 0$ $meters/second$, $b = 40$ $meters/second$, $R = 250$ $meters$ and $\sigma = \frac{\rho}{\pi R^2}$ $nodes/meter^2$. Like $\dot{\eta}(v_1)$, $\dot{\gamma}(v_1)$ is also directly proportional to the average node density σ and the transmission radius R.

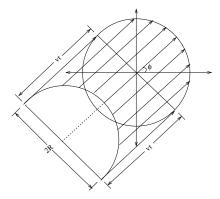## 3.6 Link Breakage Interarrival Time Distribution

Figure 8: Calculation of link breakage interarrival time distribution.

In order to derive the link breakage interarrival time distribution, we proceed in a manner similar to section 3.4. Consider Figure 8 showing the transmission zone of node 1. The shaded region $\mathbf{D_b}$ in the figure consists of all points not more than vt meters away along angle ϕ from the semicircle $\alpha \in [\frac{\pi}{2} - \phi, \frac{3\pi}{2} - \phi]$. It is easy to see that a node moving at an

[2]which is the case for any practical ad hoc or sensor network

angle ϕ can break a link with node 1 only by moving out of its transmission zone from a point on this semicircle. Given its relative velocity $\vec{v} = v \cos \phi \hat{i} + v \sin \phi \hat{j}$, a node will leave the transmission zone of node 1 within the next t seconds – and thus break the link between the two – if it is currently located in $\mathbf{D_b}$. Note that $\mathbf{D_b}$ also includes the possibility of nodes that are currently outside the transmission zone of node 1 and have yet to form a link with it.

The area of the shaded region $\mathbf{D_b}$ is $A = 2Rvt$. For given v and ϕ, the probability that the link breakage interarrival time is not more than t is equal to the probability that there is at least one node in $\mathbf{D_b}$ with velocity $\vec{v}$.

$$Prob\{link\ breakage\ interarrival\ time \leq t|v,\phi\}$$
$$= Prob\{at\ least\ one\ node\ in\ \mathbf{D_b}|v,\phi\}$$
$$= 1 - e^{-\sigma 2Rvt} \tag{28}$$

Thus, the cumulative distribution function of link breakage interarrival time is given by

$$F_{break}^{v_1}(t) = Prob\{link\ breakage\ interarrival\ time \leq t\}$$
$$= \iint\limits_{v,\phi} \left(1 - e^{-2R\sigma tv}\right) f(v,\phi) dv d\phi \tag{29}$$

The right hand sides of (24) and (29) are the same, implying that the distributions of link breakage interarrival time and new link interarrival time are the same and are given by (25). Note that, using a different argument, it was already shown in section 3.5 that the expected rate of link breakages is equal to the expected rate of new link arrivals.

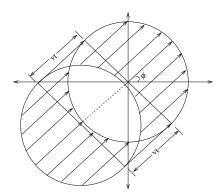## 3.7 Link Change Interarrival Time Distribution

Figure 9: Calculation of link change interarrival time distribution.

Creation of a new link or expiry of an old link constitutes a change in the set of links of a node. Given its relative velocity $\vec{v} = v \cos \phi \hat{i} + v \sin \phi \hat{j}$, the existence of a node in the shaded region $\mathbf{D_a}$ of Figure 4 will cause the formation of a new link within the next t seconds. Likewise, a node with velocity $\vec{v}$ in the shaded region $\mathbf{D_b}$ of Figure 8 will cause the breaking of a link within the next t seconds. Figure 9 shows the union of these two shaded regions, $\mathbf{D_c} = \mathbf{D_a} \cup \mathbf{D_b}$. Given $\vec{v}$, a node currently located in the shaded region $\mathbf{D_c}$ of Figure 9 will cause a link change within the next t seconds.

The area A of $\mathbf{D_c}$ can be expressed as

$$A = \begin{cases} q_1(v,t) & if\ vt \leq 2R \\ q_2(v,t) & if\ vt > 2R \end{cases} \tag{30}$$

where $q_1(v,t) = 2vtR + 2R^2\left(\sin^{-1}(\frac{vt}{2R}) + \frac{vt}{2R}\sqrt{1 - (\frac{vt}{2R})^2}\right)$ and $q_2(v,t) = 2vtR + \pi R^2$. From Assumption 5, as the nodes are assumed to be Poisson distributed,

$$Prob\{no\ node\ in\ \mathbf{D_c}|v,\phi\} = e^{-\sigma A} \tag{31}$$

Therefore, the link change interarrival time distribution is given by

$$F_{change}^{v_1}(t) = Prob\{link\ change\ interarrival\ time \leq t\}$$
$$= 1 - \iint\limits_{v,\phi} e^{-\sigma A} f(v,\phi) dv d\phi \tag{32}$$

Substituting for $f(v,\phi)$ and A and simplifying,

$$F_{change}^{v_1}(t)$$
$$= 1 - \frac{1}{\pi(b-a)}\left(\int_0^\pi \int_0^{\frac{2R}{t}} v e^{-\sigma q_1(v,t)} g(v,\phi,v_1) dv d\phi \right.$$
$$\left. + \int_0^\pi \int_{\frac{2R}{t}}^\infty v e^{-\sigma q_2(v,t)} g(v,\phi,v_1) dv d\phi \right) \tag{33}$$
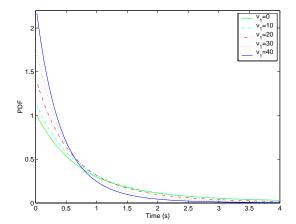

Figure 10: The link change interarrival time PDF for a node with velocity v_1.

It is not possible to explicitly evaluate the integrals in (33). The link change interarrival time density, found by differentiating (33), is plotted in Figure 10 for different node velocities v_1. $a = 0$ $meters/second$, $b = 40$ $meters/second$, $R = 250$ $meters$ and $\sigma = \frac{10}{\pi R^2}$ $nodes/meter^2$ have been used for the figure. It can be readily observed that the link change interarrival time density function decreases rapidly as time t increases. It is interesting to compare Figure 6 and Figure 10 which plot the PDFs of new link interarrival time (or link breakage interarrival time) and link change interarrival time respectively. The curves in Figure 10 appear to be scaled versions (by a factor of approximately 2, and then normalized) of the curves in Figure 6.

Although the expression for the link change interarrival time distribution in (33) looks complicated, it can be approximated by an exponential distribution function with fairly high accuracy. Using standard curve-fitting techniques, we fit the link change interarrival time density function with an exponential function of the form $f(t) = \lambda e^{-\lambda t}$. Figure 11 plots the Root Mean Squared Error (RMSE) (also known as the standard error of regression) for this fit as a function of the node velocity for the case in Figure 10. We see that the
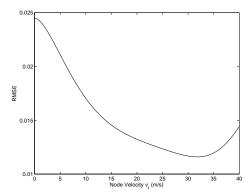
Figure 11: Root Mean Squared Error for an exponential fit to link change interarrival time density.

RMSE remains below 0.025 and is even lower at higher velocities. Similar results were obtained for other combination of parameter values, indicating a good fit.
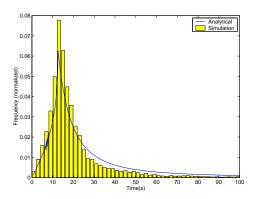
4. SIMULATIONS

Figure 12: Simulation statistics: Link Lifetime PDF for a node with velocity $v_1 = 0$ m/s.

The analytically derived expressions for the link properties have been validated by comparing them to corresponding statistics collected from simulations. Our results show that the theoretical curves are in fairly close agreement with the simulation results. Here, we present two representative plots in Figures 12 and 13 for link lifetime PDF and link change interarrival time PDF respectively.[3]

For the simulation, the network consisted of 200 nodes initially placed randomly in a square of side 1981.7 $meters$, with $R = 250$ $meters$ (implying $\sigma = \frac{10}{\pi R^2}$ $nodes/meter^2$), $a = 0$ $meters/second$ and $b = 40$ $meters/second$. The simulation duration was set to 240 $minutes$. The nodes exhibited *billiard mobility*, so that when a node reached an edge of the square simulation region, it got reflected back into the network. The small difference between the theoretical curves and the simulation statistics is attributed to the boundary effect present in the simulations. Nodes close to the boundary of the square simulation region experience fewer (or possibly, no) node arrivals from the direction of
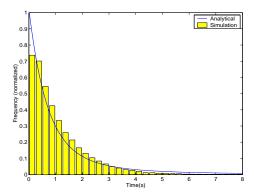
[3]Due to space constraints, comparison plots for other link properties are not included here.

Figure 13: Simulation statistics: Link change interarrival time PDF for a node with velocity $v_1 = 0$ m/s.

the boundary than otherwise expected. Also, the reflection from the boundary affects the link lifetime of the nodes close to it. We have found that experimental results fit the analytical curves better as the network size is increased while keeping the node density constant.

5. APPLICATIONS OF LINK PROPERTIES

The various properties investigated in section 3 characterize the behavior of the links of a node in a mobile environment. The derived framework can be used to design efficient algorithms for medium access, routing and transport control in ad hoc and sensor networks. It can also be used as a basis for analyzing the performance bounds of network protocols. In this section, we discuss some representative applications of the derived link properties.

The link lifetime distribution can be used to examine the stability of links in the network. Once communication starts over a link, its residual lifetime distribution can be calculated as a function of the link lifetime distribution. Mathematically, the probability density $r_T^{v_1}(t)$ of residual link lifetime given that the link has been in existence for T seconds already can be expressed as

$$r_T^{v_1}(t) = \frac{f_{link}^{v_1}(t+T)}{1 - F_{link}^{v_1}(T)} \qquad (34)$$

Here, $f_{link}^{v_1}(\cdot)$ and $F_{link}^{v_1}(\cdot)$ are the link lifetime PDF and CDF respectively, as derived in section 3.2.

The residual link lifetime density can be used to evaluate the lifetime of a route in the network. For example, consider a route with K links and let $\mathbf{X_1}, \mathbf{X_2}, \cdots, \mathbf{X_K}$ be the random variables representing each of their residual lifetimes at the time when the route is formed, given that the links have already been in existence for $T_1, T_2, \cdots, T_K$ seconds respectively. Let $\mathbf{Y}$ be a random variable representing the lifetime of the route formed by the K links. If we assume that the residual link lifetimes are independent, then the distribution $F_Y(t)$ of $\mathbf{Y}$ can be calculated as

$$
\begin{aligned}
F_Y(t) \quad = \quad & 1 - \Big[\big(1 - R_{T_1}^{v_{1_1}}(t)\big) \cdot \big(1 - R_{T_2}^{v_{1_2}}(t)\big) \cdots \\
& \qquad\qquad \cdots \big(1 - R_{T_K}^{v_{1_K}}(t)\big)\Big] (35)
\end{aligned}
$$

where $R_{T_i}^{v_{1_i}}(t)$ is the cumulative distribution function of the residual link lifetime of the ith link in the route, whose upstream node is moving with velocity v_{1_i}, given that the link

was formed T_i seconds ago. $R_{T_i}^{v_{1i}}(t)$ can be evaluated by integrating the corresponding density in (34).

The route lifetime distribution can be used to analyze the performance of routing protocols in ad hoc and sensor networks. It can also be used to provide Quality-of-Service (QoS) in the network. For example, the above framework can form the basis of schemes for selection of the most suitable set of routes for QoS techniques like Multi-Path Routing and Alternate Path Routing.

Performance of TCP in ad hoc networks is bottle-necked by its inability to adapt to link failures induced by mobility [11]. The route lifetime distribution can serve as a starting point for the estimation of the round-trip-time distribution between a source and a destination for a particular session. This could then be utilized to optimize the performance of TCP in mobile ad hoc networks.

Another application of the link properties is the optimal selection of the Time-to-Live (TTL) interval of route caches in on-demand routing protocols. For example, the work in [14] can be supplemented using the derived distributions in this paper to minimize the expected routing delay. It is also possible to develop alternate schemes to optimize other network performance metrics, if so desired.
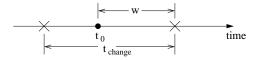

Figure 14: Time-line where the "x"-es represent the arrival of link changes and t_0 is a fixed point.

Renewal theory can be used to characterize the residual time $\mathbf{w}$ to arrival of the next link change after a given fixed instant t_0. Figure 14 shows the time-line where t_0 and $\mathbf{w}$ are indicated and the "x"-es represent the arrival of link changes. The probability density $f_w^{v_1}(w)$ of $\mathbf{w}$ is given by

$$f_w^{v_1}(w) = \dot{\gamma}(v_1)\big[1 - F_{change}^{v_1}(w)\big] \qquad (36)$$

where $\dot{\gamma}(v_1)$ and $F_{change}^{v_1}(w)$ are the expected link change arrival rate and the link change interarrival time distribution respectively, as found before. Similarly, given a fixed point t_0, the density of the residual time to arrival of the next new link or the next link breakage can be calculated by appropriately replacing the corresponding functions in (36).

The framework can also serve as the basis for a scheme to determine a node's optimal zone radius in the Independent Zone Routing (IZR) framework [21], a hybrid adaptive routing framework for mobile ad hoc networks.

Another application of the analytical framework is the design of an efficient updating strategy for proactive routing protocols. We will focus on this particular application in the next section in order to provide an illustration of the usefulness of the framework.

6. PROACTIVE UPDATING STRATEGY

Proactive or *table-driven* routing protocols for ad hoc networks maintain routes to all the nodes in the network at all times so that when a data packet needs to be forwarded, a route is known and can immediately be used. This is done by regular broadcast of routing updates reflecting changes in the network topology into the network. Examples of proactive routing protocols include DSDV [19], TBRPF [2], WRP

[17] and FSR [18]. Hybrid routing approaches like ZRP [9] also utilize a limited-scope proactive protocol (IARP) as one of its components [10].

The performance of a proactive protocol depends on the particular scheme the protocol uses to broadcast the routing updates in the network. If these updates are broadcasted too often, it may lead to wastage of resources and inefficient performance of the network. On the other hand, if these updates are broadcasted too infrequently, nodes may maintain incorrect picture of the network, possibly leading to lost packets, routing loops and delays.

In the following, we develop a strategy for broadcasting of routing updates by proactive protocols. The goal of the strategy is to reduce the amount of routing overhead in the network, while ensuring that the performance of the network does not deteriorate. This would improve the efficiency and scalability of proactive as well as hybrid protocols [22], making them better suited for the dynamic ad hoc networking environment.

6.1 Related Work

All proactive protocols broadcast periodic HELLO beacons to their neighbors. The beacons enable a node to detect the presence of a new node within its transmission zone or a loss of a link to a neighbor. Note that these beacons are in addition to the routing updates broadcasted by the proactive protocol.

There are two schemes commonly adopted by the existing proactive routing protocols to broadcast routing updates in the network. Some of the proactive protocols broadcast routing updates periodically with a fixed interval. Examples include FSR [18] and IARP [10]. The other scheme used is to broadcast an update for each detected change in the link status to a neighbor. This is sometimes associated with a default periodic update interval. Examples of this approach are DSDV [19], WRP [17] and TBRPF [2].

6.2 Motivation

Broadcasting a link-state update each time a change is detected has the potential of producing a lot of control traffic. One reason being that in a wireless environment, due to shadow and multipath fading, the radio link between mobile nodes may experience frequent disconnects and reconnects. Also, often a node's link changes may arrive quite closely spaced in time. For example, if a node starts moving all of a sudden, its links may break or new links may be created in quick succession. Thus, instead of broadcasting an update for each of the detected changes, if the node were to wait for a small amount of time before it broadcasted the next update, information about many changes can be conveyed in a single update packet. Hence, the node would save by broadcasting considerably smaller number of update packets, provided that a small delay can be tolerated by the network.

Consequently, broadcasting proactive updates involves a trade-off between the amount of control overhead and the consistency of the network topology information maintained by the nodes. Periodic updates are sometimes preferred in proactive protocols as they aggregate the information about link changes during the last interval in a single packet. However, broadcasting periodic updates at fixed intervals also has its own problems. Usually, the update interval is designed to reduce the delay in the worst case scenario – en-

abling the updates of the nodes with the most frequent link changes[4] to be obtained on time by other nodes [9]. Thus the nodes which are experiencing much less frequent changes end up broadcasting a lot of redundant updates, which could be saved, if a velocity-sensitive scheme were to be used.

With an aim to study and optimize the trade-off between aggregation of multiple link change updates in a single packet and the delay involved in dissemination of information about these link changes, we next design a proactive updating strategy.

6.3 Updating Strategy Design

In order to reduce the routing overhead, we wish to find the largest update period for periodically broadcasting link-state updates such that the expected delay between the detection of a link change and the next broadcast of the link-state is still "small" enough. In Figure 15, T_0 is the periodic update interval, the "x"-es represent detection of a link change and t_0 is the delay experienced by the first link change during an update interval before the corresponding update is broadcasted.

Thus the problem can be formulated as follows: Maximize T_0 such that the average waiting time for broadcasting the *first* link change during an update interval is bounded. In other words, *maximize T_0 such that $E(t_0) \leq \alpha$*, where α is the bound required on the mean value of the delay with which the update about the first detected change in an update interval is broadcasted. α could be considered a Quality of Service (QoS) parameter for the network performance. Thus, the delay before which a topology change in the network can be reflected in the routing tables of other nodes is dependent on α.

As justified in section 3.7, the link change interarrival time density for a node can be modeled by an exponential function. Therefore, let the link change interarrival time density for a node be $f_{change}(t) = \lambda e^{-\lambda t}$.

With the end of the last update interval as reference, let t indicate the time at which the next link change is detected by a particular node. Define $\eta = \lceil \frac{t}{T_0} \rceil$ and $\theta = \eta T_0 - t$. Hence $\theta \in [0, T_0]$. The cumulative distribution function for the random variable θ is given by

$$Prob(\theta \leq t_0) = Prob\Big(t \in \big\{[T_0 - t_0, T_0] \cup [2T_0 - t_0, 2T_0]$$
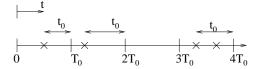$$\cup [3T_0 - t_0, 3T_0] \cup \cdots \big\}\Big)$$
$$= \sum_{k=1}^{\infty}(e^{-\lambda(kT_0 - t_0)} - e^{-\lambda kT_0})$$
$$= \frac{e^{-\lambda T_0}}{1 - e^{-\lambda T_0}}(e^{\lambda t_0} - 1) \qquad (37)$$

The probability density function of θ can be found by differentiating (37).

$$f_\theta(t_0) = \frac{e^{-\lambda T_0}}{1 - e^{-\lambda T_0}}\lambda e^{\lambda t_0} \qquad 0 \leq t_0 \leq T_0 \quad (38)$$

Therefore, the expected value of θ (or equivalently, t_0 in

Figure 15: Time-line showing the periodic updates after every interval T_0, the arrival of link changes and the residual time t_0 to the next link-state broadcast after the arrival of a link change.

Figure 15) is given by

$$E(t_0) = \frac{e^{-\lambda T_0}}{1 - e^{-\lambda T_0}}\lambda \int_0^{T_0} t' e^{\lambda t'} dt'$$
$$\Rightarrow E(t_0) = \frac{T_0}{1 - e^{-\lambda T_0}} - \frac{1}{\lambda} \leq \alpha \qquad (39)$$

Here, λ represents the mean link change rate for a node and is a function of its velocity. If the velocity of a node is known[5], λ can be calculated using (27). Alternately, a node can simply estimate it online by measuring the rate of changes in its set of links, averaged over a window. Such an estimate would adapt to any change in the node mobility as well.

Thus, we have a strategy for broadcasting the routing updates. Given the value of the bound α and the adaptively estimated link change arrival rate λ, the maximum value of T_0 which satisfies (39) is calculated at the start of an update interval. If at least one link change is detected during the update interval, a routing update is broadcasted. If no link changes are detected, no update is broadcasted, reducing the overhead. Additionally, an update is broadcasted if the node has not broadcasted any updates in the last MAX_IDLE_SLOTS intervals. Broadcasting an update at least every MAX_IDLE_SLOTS is used as a protection against transmission errors and loss of soft state.

Note that this strategy determines the generation of a new update by a node. The nodes receiving the broadcasted update would still need to forward them in the network according to the rules of the particular proactive protocol being used.

6.4 Performance Evaluation

The performance of the derived strategy is evaluated using simulations. A link-state based proactive routing protocol, as described in [10], is utilized. The network consists of 50 nodes spread randomly in a square of side $990.8\ meters$. The transmission radius of the nodes is set to $R = 250\ meters$, so that the node density turns out to be $\sigma = \frac{10}{\pi R^2}$. A node moves at a constant speed v which is chosen from a uniform distribution between $a = 0\ meters/second$ and $b = 40\ meters/second$. It is assigned an initial direction θ, which is uniformly distributed between 0 and 2π. When a node reaches an edge of the simulation region, it is reflected back into the network such that the angle of incidence equals the angle of reflection (*Billiard Mobility*). Each node initiates a session with a randomly chosen destination and sends an average of 5 packets. The number of packets in a particular session is *Poisson* distributed and the interarrival delay

---

[4]The link change rate for a node as a function of its velocity is plotted in Figure 7.

[5]provided by, for example, GPS

154

between sessions for a particular node is exponentially distributed with a mean of 2.5 *seconds*. The simulation duration is set to 300 *seconds*. The traces for mobility and session statistics are kept the same for different simulation runs. The simulations are performed in the $OPNET^{TM}$ simulation environment. No data is collected for the first 5 simulation seconds to allow the initial route discovery process to stabilize. The parameter MAX_IDLE_SLOTS was set to 50 for the simulations.

The proposed strategy is compared to the two commonly used updating schemes in existing proactive protocols, as described in section 6.1.

- **Change-Triggered:** A node broadcasts an update whenever a link change is detected. If no broadcasts have been made in the last $BROADCAST\_TIMEOUT = 5$ *seconds*, the node broadcasts an update.

- **Periodic:** All nodes broadcast their link-states every $T_{periodic}$ seconds. This period is computed using $T_{periodic} = \frac{3R/20}{v_m}$ [9], where v_m is the maximum velocity of the nodes in the network and R is the transmission radius.
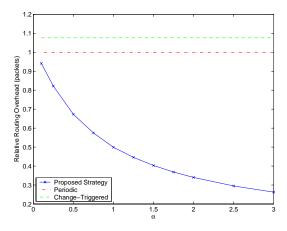

Figure 16: Total routing overhead (packets) relative to Periodic updating as a function of the bound α.
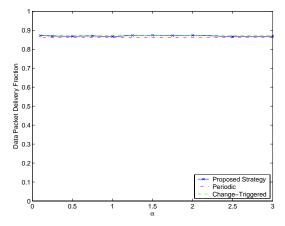

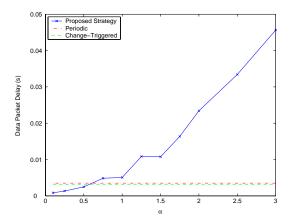**Figure 17: Data packet delivery fraction as a function of the bound α.**

Figure 18: Data packet delivery delay as a function of the bound α.

Figure 16 plots the total routing overhead generated in the network for the proposed strategy as a function of the parameter α that bounds the mean delay involved in broadcasting a routing update. The routing overhead is measured in terms of the number of packets transmitted and is shown relative to the overhead associated with the Periodic updating scheme. As can be observed from the figure, the proposed strategy leads to significant reduction in the routing overhead as compared to the Periodic or the Change-Triggered schemes, especially for values of $\alpha \geq 0.5$. Reduction in overhead for a routing protocol is an important goal as it translates to lower power consumption, lesser congestion, reduced memory and processing requirements, and easier access to the communication channel. This increases the efficiency and scalability of the protocol.

Figure 17 shows that the fraction of data packets delivered to the destination remains high for the values of α considered. At the same time, the delay involved in delivering the data packets to the destination increases as α is increased, as observed from Figure 18. This is due to the high amount of redundancy in routing information maintained by a link-state routing protocol. As each node has complete topology information about the network, when a data packet encounters a broken link, it is usually able to find an alternate path to the destination[6]. Thus, the data packet delivery fraction remains high even for larger values of α. However, larger values of α imply that the nodes may have more stale routing information, increasing the likelihood of the data packets encountering broken links. This leads to the data packets possibly being re-routed along alternate paths, increasing the effective path length, and thus increasing the latency.

Hence, considerable reduction in routing overhead can be obtained by choosing an appropriate value of α depending on the quality of service needed from the network. For example, setting $\alpha = 1$ reduces the routing overhead by more than 50% as compared to Periodic or Change-Triggered updating, while keeping the data packet delivery fraction high and increasing the data packet delay only marginally. For $\alpha = 0.5$, the reduction in routing overhead is more than 33% (as compared to Periodic or Change-Triggered updating), the data packet delay also reduces and the data packet delivery fraction remains high. Even bigger savings in routing

---

[6]given that the network is fairly well-connected

overhead can be obtained if some latency can be tolerated by the application layer.

7. CONCLUSIONS

Developing efficient algorithms for communication in multi-hop environments like ad hoc and sensor networks is challenging, particularly due to the mobility of nodes forming the network. An attempt has been made in this paper to develop an analytical framework that can provide a better understanding of network behavior under mobility. We derive expressions for a number of properties characterizing the creation, lifetime and expiration of communication links in the network.

The developed framework can serve as the starting point for performance evaluation and optimization of existing protocols for mobile ad hoc and sensor networks. It can also be used for designing efficient communication schemes for these networks. This has been illustrated by the discussion on some potential applications of the derived link properties. We choose one of the applications and design an updating strategy for proactive routing protocols. The proposed strategy bounds the delay involved in dissemination of an update about a link change, while reducing the routing overhead. This leads to significant performance improvements in terms of savings in routing overhead, while maintaining high data packet delivery ratio and acceptable latency.

While the node behavior in certain real world environments may be different from how it is modeled here, the developed framework can still serve to provide an indication of the bounds on network behavior. Further, the techniques employed could be used to derive link properties under different assumptions on node behavior as well.

8. REFERENCES

[1] S. Agarwal, A. Ahuja, J.P. Singh, R. Shorey, "Route-lifetime Assessment Based Routing (RABR) Protocol for Mobile Ad-hoc Networks," *ICC 2000*, vol. 3, pp.1697 - 1701, New Orleans.

[2] B. Bellur, R.G. Ogier, "A Reliable, Efficient Topology Broadcast Protocol for Dynamic Networks," *IEEE INFOCOM,* March 1999.

[3] C. Bettstetter, H. Hartenstein, X. Perez-Costa, "Stochastic Properties of the Random Waypoint Mobility Model," *ACM/ Kluwer Wireless Networks,* to appear 2004.

[4] C. Bettstetter, G. Resta, P. Santi, "The Node Distribution of the Random Waypoint Mobility Model for Wireless Ad Hoc Networks," *IEEE Transactions on Mobile Computing*, vol. 2, no. 3, July-Sept. 2003.

[5] T. Camp, J. Boleng, V. Davies, "A Survey of Mobility Models for Ad Hoc Network Research," *Wireless Communication & Mobile Computing (WCMC)*, vol. 2, no. 5, pp. 483-502, 2002.

[6] R. Dube, C. Rais, K.-Y. Wang, S. Tripathi, "Signal stability based adaptive routing (SSA) for ad hoc networks," *IEEE Personal Communications*, Feb. 1997.

[7] M. Gerharz, C. de Waal, M. Frank, P. Martini, "Link Stability in Mobile Wireless Ad Hoc Networks," *IEEE LCN'02*, Nov. 2002, Tampa, Florida.

[8] A.J. Goldsmith, S.B. Wicker, "Design challenges for energy-constrained ad hoc wireless networks," *IEEE Wireless Communications*, vol. 9, no. 4, Aug. 2002.

[9] Z.J. Haas, M.R. Pearlman, "The Performance of Query Control Schemes for the Zone Routing Protocol," *IEEE/ACM Transactions on Networking*, Aug. 2001.

[10] Z.J. Haas, M.R. Pearlman, P. Samar, "The Intrazone Routing Protocol (IARP) for Ad Hoc Networks," *IETF MANET,* Internet Draft, July 2002.

[11] G.D. Holland, N.H. Vaidya, "Analysis of TCP performance over mobile ad hoc networks," *ACM MobiCom 1999*, Aug. 1999.

[12] Y.-C. Hu, D.B. Johnson, "Caching Strategies in On-Demand Routing Protocols for Wireless Ad Hoc Networks," *ACM MobiCom 2000*, Boston, Aug., 2000.

[13] S. Jiang, D.J. He, J.Q. Rao, "A prediction-based link availability estimation for mobile Ad Hoc networks," *IEEE INFOCOM 2001*, Anchorage, April, 2001.

[14] B. Liang, Z.J. Haas, "Optimizing Route-Cache Lifetime in Ad Hoc Networks," *IEEE INFOCOM 2003*, San Francisco, April, 2003.

[15] A.B. McDonald, T.F. Znati, "A mobility-based framework for adaptive clustering in wireless ad hoc networks," *IEEE JSAC*, 17(8), Aug. 1999.

[16] J.P. Mullen, "Robust Approximations to the Distribution of Link Distances in a Wireless Network Occupying a Rectangular Region," *Mobile Computing and Communications Review*, Vol. 7, No. 2, April 2003.

[17] S. Murthy, Garcia-Luna-Aceves, "An Efficient Routing Protocol for Wireless Networks," *Mobile Networks and Applications*, 1(2), 1996.

[18] G. Pei, M. Gerla, T.-W. Chen, "Fisheye State Routing: A Routing Scheme for Ad Hoc Wireless Networks," *ICC 2000*, New Orleans, LA, June 2000.

[19] C. Perkins, P. Bhagwat, "Highly Dynamic Destination Sequenced Distance Vector Routing (DSDV) for Mobile Computers," *ACM SIGCOMM,* Oct. 1994.

[20] N. Sadagopan, F. Bai, B. Krishnamachari, A. Helmy, "PATHS: Analysis of PATH Duration Statistics and their Impact on Reactive MANET Routing Protocols," *MobiHoc 2003*, Annapolis, MD, June 2003.

[21] P. Samar, M.R. Pearlman, Z.J. Haas, "Independent Zone Routing: An Adaptive Hybrid Routing Framework for Ad Hoc Wireless Networks," IEEE/ ACM Transactions on Networking, Aug. 2004 (expected).

[22] P. Samar, M.R. Pearlman, Z.J. Haas, "Hybrid Routing: The Pursuit of an Adaptable and Scalable Routing Frame-work for Ad Hoc Networks," *Ad hoc Wireless Networking*, X. Cheng, X. Huang and D.-Z. Du (eds.), Kluwer Academic Publishers, Nov. 2003.

[23] P. Samar, S.B. Wicker, "Link Dynamics in a Multi-Hop Mobile Environment," under submission.

[24] W. Su, S.-J. Lee, M. Gerla, "Mobility Prediction and Routing in Ad Hoc Wireless Networks," *International Journal of Network Management*, Jan.-Feb. 2001.

[25] C.-K. Toh, "Associativity-based Routing for Ad Hoc Networks," *Wireless Personal Comm.*, Mar. 1997.

[26] D. Turgut, S.K. Das, M. Chatterjee, "Longevity of Routes in Mobile Ad hoc Networks," *VTC Spring 2001*, Rhodes, Greece, May, 2001.

[27] J. Yoon, M. Liu, B. Noble, "Random Waypoint Considered Harmful," *IEEE INFOCOM 2003*, San Francisco, CA, April 2003.